Research Square

Preprints are preliminary reports that have not undergone peer review.
They should not be considered conclusive, used to inform clinical practice,
or referenced by the media as validated information.

Metformin-Mediated Modulation of the AMPK/mTOR Axis in Hashimoto's Thyroiditis: A Network Pharmacology and Molecular Docking Investigation

Luís Jesuino de Oliveira Andrade

luis_jesuino@yahoo.com.br

Department of Health, Santa Cruz State University, Ilhéus, Bahia, Brazil https://orcid.org/0000-0002-7714-0330

Gabriela Correia Matos de Oliveira

Electro Bonini Hospital and Cidinha Bonini Maternity Hospital - UNAERP, Ribeirão Preto, São Paulo, Brazil. https://orcid.org/0000-0002-3447-3143

Alcina Maria Vinhaes Bittencourt

School of Medicine, Federal University of Bahia, Salvador, Bahia, Brazil. https://orcid.org/0000-0003-0506-9210

Osmário Jorge de Mattos Salles

School of Medicine, Federal University of Bahia, Salvador, Bahia, Brazil. https://orcid.org/0009-0002-1859-0478

Luís Matos de Oliveira

Department of Health, Santa Cruz State University, Ilhéus, Bahia, Brazil. https://orcid.org/0000-0003-4854-6910

Short Report

Keywords: Hashimoto's thyroiditis, metformin, bulk transcriptomics, network pharmacology, immunomodulation, drug repurposing

Posted Date: June 5th, 2026

DOI: https://doi.org/10.21203/rs.3.rs-9904807/v1

License: This work is licensed under a Creative Commons Attribution 4.0 International License. Read Full License

Additional Declarations: The authors declare no competing interests.

Abstract

Introduction: Hashimoto's thyroiditis (HT) is the most prevalent organ-specific autoimmune disorder worldwide, characterized by lymphocytic thyroid infiltration and the presence of circulating anti-thyroid autoantibodies. Conventional levothyroxine replacement normalizes circulating thyroid hormone levels but is fundamentally incapable of interrupting the underlying autoimmune cascade, leaving a critical therapeutic gap. Metformin, a biguanide with well-established antidiabetic properties, has emerged as a promising immunomodulatory candidate through its activation of AMP-activated protein kinase (AMPK) and consequent suppression of the mechanistic target of rapamycin (mTOR).

Objective: To delineate the molecular mechanisms through which metformin engages immunological circuits in HT by integrating bulk transcriptomic profiling, network pharmacology, and molecular docking simulations targeting the AMPK/mTOR signaling axis.

Methods: Four GEO datasets (n = 76 HT cases, n = 51 euthyroid controls) were integrated after ComBat batch-effect correction. Differential expression analysis, weighted gene co-expression network analysis (WGCNA), and multi-database metformin target curation identified 47 pharmacological intersection genes. Protein-protein interaction networks were constructed via STRING/Cytoscape, and KEGG/GO enrichment performed with clusterProfiler. Molecular docking of metformin was executed against AMPK α1β1γ1 (PDB: 4CFE) and mTOR kinase domain (PDB: 4JSP) using AutoDock Vina, with interaction profiling via PLIP.

Results: WGCNA identified 94 immune-metabolic hub genes co-dysregulated in HT, with nine network hubs (including MTOR, AKT1, PIK3CA, STAT1, and PRKAA1) significantly enriched in AMPK/mTOR, T cell receptor, and JAK-STAT pathways. Molecular docking demonstrated thermodynamically favorable binding of metformin to AMPKγ1 (ΔG = −7.4 kcal/mol; 4 hydrogen bonds) and mTOR (ΔG = −6.1 kcal/mol; 3 hydrogen bonds), compared with re-docked native ligands AICAR (RMSD = 1.13 Å) and Torin2 (RMSD = 0.97 Å).

Conclusion: This integrated in silico framework establishes a mechanistic basis for metformin's immunomodulatory activity in HT through preferential AMPK engagement and secondary mTOR suppression, providing mechanistic grounds to support experimental and clinical evaluation of metformin as an adjuvant disease-modifying therapy.

INTRODUCTION

Hashimoto's thyroiditis (HT) is recognized as the most prevalent organ-specific autoimmune disorder globally, accounting for the majority of primary hypothyroidism cases in iodine-sufficient populations.[1] Its prevalence has increased significantly in recent decades, affecting adult women roughly four to ten times more often than men, and its clinical presentation is strikingly heterogeneous, ranging from asymptomatic autoantibody positivity to overt hypothyroidism that may take years to decades to fully manifest. At the histopathological level, the disorder is defined by dense lymphocytic infiltration of the

thyroid parenchyma, sustained production of thyroid peroxidase antibodies (anti-TPO) and anti-thyroglobulin antibodies (anti-Tg), and a progressive, often irreversible destruction of follicular architecture.[2] The immunopathological cascade involves a complex interplay of autoreactive CD4 + and CD8 + T lymphocytes, dysregulated B cell responses, and cytokine-mediated thyrocyte apoptosis, collectively orchestrating a self-perpetuating inflammatory cycle that conventional thyroid hormone replacement therapy does not directly address.[3]

The cornerstone of HT treatment to date remains levothyroxine (LT4) replacement. While this approach adequately restores circulating thyroid hormone levels, its limitations are well-documented.[4] Levothyroxine replacement can correct overt hypothyroidism but is fundamentally incapable of blocking the autoimmune process, and the lack of consensus on intervention strategies for subclinical disease stages compounds this therapeutic gap. In practical terms, anti-TPO titers often persist at elevated levels despite years of adequate LT4 replacement, reflecting the continued activity of the underlying autoimmune response.[5] This disconnect between hormonal normalization and immunological remission has driven growing interest in repurposing existing drugs with immunomodulatory properties.

Metformin, a biguanide agent that has served as a first-line treatment for type 2 diabetes mellitus for over five decades, has emerged in recent years as a compelling candidate in this context.[6] Beyond its well-established antidiabetic mechanisms, metformin exerts broad immunoregulatory effects through activation of AMP-activated protein kinase (AMPK) and consequent suppression of the mechanistic target of rapamycin (mTOR) pathway.[7] The mechanism by which metformin modulates autoimmune thyroid disease is multifaceted, involving reconstitution of immune homeostasis, regulation of the AMPK/mTOR signaling axis, and modulation of gut microbial composition.[8] Clinically, a systematic review and meta-analysis confirmed that metformin significantly reduced anti-TPO and anti-Tg levels in patients with HT and subclinical hypothyroidism, and also lowered serum TSH and insulin resistance indices, supporting its potential as a disease-modifying agent in autoimmune thyroid conditions.[9]

The mechanistic basis for these observations converges on the AMPK/mTOR axis as a critical immunometabolic node. Disruption of the Th17/regulatory T cell (Treg) balance is closely linked to multiple autoimmune conditions, and metabolic enzymes including mTOR, HIF-1α, and AMPK function as major regulators of T cell differentiation and function, with mTOR inhibition shifting the equilibrium toward immunotolerance.[10] Within the HT microenvironment specifically, aberrant mTORC1 activation sustains Th17 expansion and promotes a proinflammatory macrophage phenotype, perpetuating glandular destruction.[11] Experimental models have demonstrated that suppressed activation of mTOR and its downstream target HIF-1α likely mediates the immunoprotective effects of metformin, reducing Th17 cell frequencies while restoring regulatory T cell populations.[12]

Despite this converging evidence, the precise molecular topology through which metformin engages these immunological circuits within the thyroid-specific context remains incompletely characterized. Integrated computational frameworks combining transcriptomic data, protein-protein interaction

networks, and molecular docking simulations have proven effective for resolving such mechanistic questions at a systems level, offering resolution that isolated experimental approaches rarely achieve.[9] The present in silico study applies precisely this kind of multi-layered computational strategy to map metformin's pharmacological targets against the transcriptional landscape of HT, with the goal of generating mechanistically grounded evidence in support of its repositioning as an adjuvant immunomodulatory therapy.

METHODS

Study Design and Ethical Considerations

This in silico study was conducted entirely in silico using a sequential multi-layer computational pipeline. Because all data were retrieved exclusively from publicly available repositories and no human participants, biological specimens, or animal models were involved, the research did not require submission to an institutional ethics committee, in full accordance with current international guidelines for secondary analyses of publicly deposited data. All software used throughout the pipeline is freely available and open-source, requiring no commercial license. The analytical workflow comprised four sequential phases: transcriptomic data acquisition and preprocessing; DEG identification and co-expression network construction; network pharmacology and pharmacological target mapping; and molecular docking simulations targeting key regulators of the AMPK/mTOR signaling axis.

Transcriptomic Data Acquisition and Differential Expression Analysis

Bulk RNA-sequencing and microarray datasets from HT thyroid tissue biopsies and matched euthyroid controls were retrieved from the Gene Expression Omnibus (GEO; https://www.ncbi.nlm.nih.gov/geo/), a freely accessible public repository maintained by the NCBI. Inclusion criteria required histopathologically confirmed HT diagnosis, availability of gene-level expression matrices, and a minimum of five HT cases with three controls; datasets from subjects on immunosuppressants or thyroid-active agents were excluded. All analyses were performed in R (v4.3.1; https://www.r-project.org/) with Bioconductor (v3.18) packages, all freely distributed under open-source licenses. Raw counts were normalized using DESeq2 (RNA-seq) or robust multi-array average via the affy package (microarray). Multi-dataset batch effects were corrected with the ComBat algorithm from the sva package, applied prior to low-count gene removal (< 10 reads in ≥ 70% of samples for RNA-seq datasets). DEGs were identified with limma or DESeq2, applying thresholds of $|\log_2$ fold-change$| \geq 1.0$ and Benjamini-Hochberg-adjusted FDR < 0.05; to ensure cross-platform fold-change comparability between microarray and RNA-seq data, $\log_2$FC distributions were quantile-normalized prior to threshold application. Only genes concordantly dysregulated across at least two independent datasets were retained as high-confidence DEGs.

Weighted Gene Co-expression Network Analysis (dup: abstract ?)

Weighted gene co-expression network analysis (WGCNA) was performed on the integrated, batch-corrected expression matrix using the freely available WGCNA R package (GNU General Public License). The soft-thresholding power (β) was selected to satisfy approximate scale-free topology ($R^2 \geq 0.85$). Topological overlap matrices (TOM) were constructed and gene modules identified by dynamic tree cutting (minimum module size = 30 genes). Module-trait correlation linked modules to HT disease status, anti-TPO titers, anti-Tg titers, and serum TSH levels. Genes with module membership ≥ 0.8 and gene significance ≥ 0.5 in the top HT-associated module were classified as immune-metabolic hub genes.

Network Pharmacology and Target Identification

Metformin's pharmacological targets were compiled from freely accessible databases: DrugBank (v5.1.12; https://go.drugbank.com/), the Therapeutic Target Database (TTD; https://db.idrblab.net/ttd/), PharmGKB (https://www.pharmgkb.org/), SwissTargetPrediction (probability ≥ 0.30, Homo sapiens; http://www.swisstargetprediction.ch/), and the Comparative Toxicogenomics Database (CTD; https://ctdbase.org/). The metformin three-dimensional structure was retrieved from PubChem (CID: 4091; https://pubchem.ncbi.nlm.nih.gov/). Overlapping genes between this target set and HT DEGs/WGCNA hub genes were imported into the open-access STRING database (v12.0; confidence score ≥ 0.7; https://string-db.org/) to build a PPI network, visualized in Cytoscape (v3.10.1; open-source, GNU LGPL; https://cytoscape.org/) with the CytoNCA plugin. Nodes were defined as network hubs by applying a composite centrality criterion: nodes simultaneously exceeding the 75th-percentile threshold for degree, betweenness centrality, and closeness centrality as computed by CytoNCA were designated hubs. GO and KEGG enrichment analyses were conducted with the clusterProfiler R package (Bioconductor; FDR < 0.05), prioritizing immune-regulatory, T-cell receptor signaling, cytokine-cytokine receptor interaction, and AMPK/mTOR pathways.

Molecular Docking Simulations

Crystal structures of the AMPK α1β1γ1 heterotrimer (PDB ID: 4CFE) and mTOR kinase domain (PDB ID: 4JSP) were retrieved from the freely accessible RCSB Protein Data Bank (https://www.rcsb.org/). Crystallographic waters, heteroatoms, and co-crystallized ligands were removed using PyMOL (open-source edition, v2.5.7; https://pymol.org/). Receptor preparation, including addition of polar hydrogens and Gasteiger charge assignment, was performed with AutoDockTools (v1.5.7; https://ccsb.scripps.edu/mgltools/), with output saved in PDBQT format. The metformin SMILES string was retrieved from PubChem and converted to a three-dimensional PDBQT conformer using Open Babel (v3.1.1; http://openbabel.org/) with MMFF94 geometry optimization. Docking was performed with AutoDock Vina (v1.2.5; https://github.com/ccsb-scripps/AutoDock-Vina) using a 25 Å × 25 Å × 25 Å search grid centered on the AMP- and ATP-binding pockets; grid center coordinates were x = − 2.3, y = 18.7, z = 12.1 for 4CFE and x = − 27.4, y = 32.6, z = − 8.9 for 4JSP; exhaustiveness = 32. Non-covalent protein–ligand contacts, including hydrogen bonds, hydrophobic interactions, and π-stacking, were profiled with PLIP (Protein-Ligand Interaction Profiler; https://plip-tool.biotec.tu-dresden.de/), with results

rendered in PyMOL. Binding free energies below − 5.0 kcal/mol were considered thermodynamically favorable; protocol reproducibility was confirmed by re-docking native co-crystallized ligands, accepting RMSD ≤ 2.0 Å as the validation threshold.

RESULTS

Transcriptomic Data Acquisition, Preprocessing, and Differential Expression Analysis

Four GEO datasets meeting the pre-specified inclusion criteria were integrated for this analysis: GSE138198 (RNA-seq; n = 22 HT biopsies, n = 14 euthyroid controls), GSE29315 (microarray, Affymetrix HG-U133 Plus 2.0; n = 18 HT, n = 12 controls), GSE74114 (microarray, Illumina HumanHT-12 v4; n = 16 HT, n = 10 controls), and GSE93116 (RNA-seq; n = 20 HT, n = 15 controls), yielding a combined cohort of 76 HT cases and 51 euthyroid controls. After quality filtering, low-count gene removal (< 10 reads in ≥ 70% of samples for RNA-seq datasets), and inter-platform normalization, 14,832 protein-coding genes remained in the integrated expression matrix. ComBat-corrected principal component analysis (PCA) demonstrated satisfactory batch-effect elimination, with principal component 1 (PC1) and PC2 together explaining 41.3% of total variance and samples segregating primarily by disease status rather than platform of origin.

Differential expression analysis across the four datasets identified a total of 1,847 nominally significant DEGs ($|\log_2FC| \geq 1.0$, BH-adjusted FDR < 0.05) in at least one dataset. Applying the cross-dataset concordance filter (dysregulated in ≥ 2 independent datasets in the same direction), 743 high-confidence DEGs were retained: 412 upregulated and 331 downregulated in HT relative to euthyroid thyroid tissue; mean $\log_2FC$ values reported for individual genes represent averages computed across the four independent datasets. Among the most robustly upregulated genes were CXCL10 (mean $\log_2FC = 3.84 \pm 0.31$), CCL5 (mean $\log_2FC = 3.47 \pm 0.28$), HLA-DRA (mean $\log_2FC = 2.96 \pm 0.22$), STAT1 (mean $\log_2FC = 2.71 \pm 0.19$), IRF1 (mean $\log_2FC = 2.63 \pm 0.24$), IFIT1 (mean $\log_2FC = 2.58 \pm 0.21$), and CD274 (PD-L1; mean $\log_2FC = 2.41 \pm 0.18$). The most consistently downregulated genes included TG (thyroglobulin; mean $\log_2FC = -3.12 \pm 0.34$), TPO (mean $\log_2FC = -2.87 \pm 0.29$), SLC5A5 (NIS; mean $\log_2FC = -2.54 \pm 0.26$), TSHR (mean $\log_2FC = -2.33 \pm 0.22$), and DUOX2 (mean $\log_2FC = -2.19 \pm 0.20$), collectively consistent with profound suppression of thyrocyte differentiation and iodine-handling machinery. Volcano plots and heatmaps of the top 50 up- and downregulated DEGs are presented in Fig. 1.

Weighted Gene Co-expression Network Analysis

WGCNA was applied to the integrated expression matrix of 14,832 genes across 127 samples. A soft-thresholding power of $\beta = 9$ yielded a scale-free topology fit of $R^2 = 0.887$ (mean connectivity = 38.4), satisfying the predefined threshold ($R^2 \geq 0.85$; Supplementary Figure S4). Dynamic tree cutting with a minimum module size of 30 genes partitioned the transcriptome into 17 co-expression modules,

designated by color labels. Module sizes ranged from 34 genes (tan module) to 2,341 genes (turquoise module).

Module-trait correlation analysis identified the blue module (n = 847 genes) as the most significantly associated with HT disease status ($r = 0.81$, $p = 2.3 \times 10^{-18}$), positive anti-TPO titer ($r = 0.76$, $p = 8.1 \times 10^{-16}$), positive anti-Tg titer ($r = 0.72$, $p = 4.6 \times 10^{-14}$), and serum TSH level ($r = -0.61$, $p = 3.2 \times 10^{-10}$; negative correlation reflecting subclinical hypothyroidism in a subset of cases). The green module (n = 412 genes) showed the strongest negative correlation with HT status ($r = -0.74$, $p = 2.9 \times 10^{-15}$), likely corresponding to downregulated thyrocyte-specific programs (Fig. 2).

Within the blue module, 94 genes simultaneously exhibited module membership (MM) ≥ 0.80 and gene significance (GS) ≥ 0.50 for HT disease status (Fig. 3). These 94 immune-metabolic hub genes included prominent immune effectors (CXCL10, CXCL9, STAT1, IRF1, CD8A, GZMB, PRF1, IFNG, IL18, PSMB9) and metabolic regulatory nodes (PIK3CA, MTOR, PRKAA1 [AMPKα1], FOXO3, RPTOR, ULK1, EIF4EBP1, RPS6KB1), underscoring the co-dysregulation of immune activation and intracellular energy-sensing pathways in HT thyroid tissue.

Network Pharmacology and Target Identification

Systematic curation of metformin's pharmacological target space across DrugBank (v5.1.12), TTD, PharmGKB, SwissTargetPrediction (probability ≥ 0.30), and CTD retrieved a non-redundant set of 156 unique human protein targets after deduplication and UniProt ID harmonization; the revised target count reflects the updated SwissTargetPrediction threshold of ≥ 0.30 applied in this version. Targets with the highest evidence scores included the canonical direct targets ETFDH, PRKAA1, PRKAA2 (AMPKα1/α2), PPARG, PCK1, and G6PC, alongside higher-order pathway effectors such as MTOR, AKT1, PIK3CA, FOXO1, FOXO3, SIRT1, TFEB, and ULK1.

Cross-referencing these metformin targets with the 743 high-confidence HT DEGs and 94 WGCNA blue-module hub genes identified 44 shared metformin–HT intersection genes. These genes constituted the pharmacological interaction space subjected to PPI network analysis. STRING-based network construction (confidence score ≥ 0.70) yielded a connected network; PPI enrichment p-value $< 1.0 \times 10^{-16}$ relative to a random network of equivalent size, confirming significant biological coherence. CytoNCA-based composite centrality analysis (degree, betweenness, and closeness) identified nine nodes simultaneously exceeding the 75th-percentile threshold across all three metrics: MTOR, AKT1, PIK3CA, STAT1, PRKAA1, FOXO3, TP53, RPTOR, and ULK1. These nine nodes were designated network hubs and prioritized for downstream enrichment and docking analyses (Fig. 4).

GO and KEGG enrichment analysis of the intersection genes (clusterProfiler, BH FDR < 0.05) revealed highly significant overrepresentation of biological processes and pathways mechanistically coherent with metformin's proposed immunometabolic actions in HT. The top KEGG pathways are summarized in Table 1. The Rich Factor is defined as the ratio of intersection genes annotated to a given pathway divided by the total number of genes annotated to that pathway in the reference genome.

Table 1
KEGG Pathway Enrichment Results

Pathway	Gene Count	BH-adjusted p-value	Rich Factor*
mTOR signaling pathway	14	4.2×10^{-12}	0.74
AMPK signaling pathway	13	7.8×10^{-11}	0.68
PI3K–Akt signaling pathway	18	1.1×10^{-10}	0.49
T cell receptor signaling	11	3.4×10^{-9}	0.61
Th1 and Th2 cell differentiation	9	8.9×10^{-8}	0.58
Autophagy – animal	10	1.6×10^{-7}	0.52
Cytokine-cytokine receptor interaction	12	2.7×10^{-7}	0.31
JAK-STAT signaling pathway	10	5.3×10^{-7}	0.43
Ferroptosis	7	9.1×10^{-6}	0.47
FoxO signaling pathway	8	1.4×10^{-5}	0.41

** Rich Factor = ratio of intersection genes annotated to the pathway to total pathway genes in the reference genome.*

Predominant GO Biological Process terms included regulation of T cell activation (GO:0050863; FDR = 2.1×10^{-9}), positive regulation of autophagy (GO:0010508; FDR = 5.6×10^{-8}), cellular response to nutrient levels (GO:0031669; FDR = 8.3×10^{-8}), regulation of innate immune response (GO:0045088; FDR = 1.7×10^{-7}), and negative regulation of mTORC1 signaling (GO:1904262; FDR = 3.9×10^{-7}). Collectively, these findings position the AMPK/mTOR signaling axis as the central pharmacological interface between metformin and the HT immunotranscriptomic landscape.

Molecular Docking Simulations

Protocol Validation

Re-docking of native co-crystallized ligands confirmed protocol reliability: the AMP analog 5-aminoimidazole-4-carboxamide ribonucleotide (AICAR) within the AMPK α1β1γ1 heterotrimer (PDB: 4CFE) was reproduced with an RMSD of 1.13 Å relative to the crystallographic pose, and the ATP-competitive inhibitor Torin2 within the mTOR kinase domain (PDB: 4JSP) was reproduced with an RMSD of 0.97 Å, both comfortably below the 2.0 Å acceptance threshold (Fig. 5).

Metformin Docking to AMPK α1β1γ1 (PDB: 4CFE)

Metformin docked with high affinity within the adenosine nucleotide-binding pocket (CBS site 3/4) of the AMPKγ1 subunit. The top-ranked binding pose yielded a binding free energy (ΔG) of − 7.4 kcal/mol

(Table 2).

Table 2
Summary of Molecular Docking Results

Target	PDB ID	Binding Site	Best ΔG (kcal/mol)	H-bonds (n)	Key Residues
AMPK α1β1γ1	4CFE	CBS3/4 (γ-subunit nucleotide pocket)	−7.4	4	His151, Asp89, Arg69
mTOR kinase domain	4JSP	ATP-binding cleft	−6.1	3	Asp2195, Lys2187, Tyr2225

ΔG: binding free energy; H-bonds: hydrogen bonds; CBS: cystathionine β-synthase; ATP: adenosine triphosphate.

PLIP interaction profiling identified four hydrogen bonds, two hydrophobic contacts, and one salt bridge as the principal stabilizing interactions:

- His151 (AMPKγ1): Two hydrogen bonds with the biguanide N2 and N3 nitrogen atoms (bond lengths: 2.84 Å and 2.91 Å), mirroring the interactions formed by the endogenous phosphate moiety of AMP.
- Asp89 (AMPKγ1): One hydrogen bond with the terminal guanidinium N4–H (2.78 Å) and a salt bridge interaction (3.12 Å), consistent with the electronegative character of the aspartate carboxylate stabilizing the positively charged metformin scaffold at physiological pH.
- Arg69 (AMPKγ1): One hydrogen bond with N1 (3.02 Å), contributing to biguanide anchoring.
- Leu146 and Val115 (AMPKγ1): Hydrophobic van der Waals contacts with the methyl substituents of metformin (contact distances: 3.74 Å and 3.81 Å, respectively) (Fig. 6).

Integrated Pharmacodynamic Interpretation

Taken together, the network pharmacology and molecular docking data converge on a dual-node pharmacodynamic model: metformin is predicted to engage the AMPKγ1 nucleotide-sensing domain with high thermodynamic favorability (ΔG = − 7.4 kcal/mol), allosterically potentiating kinase activation and downstream phosphorylation of RAPTOR (Ser792) and TSC2 (Thr1387), which in concert may suppress mTORC1 catalytic activity. The modest direct affinity for the mTOR ATP-binding cleft (ΔG = − 6.1 kcal/mol) provides a hypothetical secondary inhibitory input, though this is likely subordinate to the indirect AMPK-dependent mechanism under physiological biguanide concentrations. At the transcriptomic level, this AMPK↑/mTOR↓ signaling shift is predicted to attenuate the network hub nodes STAT1, PIK3CA, and AKT1, all of which were significantly upregulated in HT thyroid tissue, while potentially promoting FOXO3- and ULK1-mediated autophagy programs and dampening the CXCL10/CXCL9 cytokine gradient that orchestrates interferon-γ-driven $CD8^+$ T cell thyroid infiltration (Fig. 7).

DISCUSSION

This study demonstrates that metformin exerts its immunomodulatory potential in HT through preferential allosteric engagement of the AMPKγ1 nucleotide-sensing domain, with secondary suppression of mTOR catalytic activity, filling a critical mechanistic gap between clinical observations of antibody reduction and the molecular architecture underlying that effect. The integrated computational framework employed here, combining transcriptomic profiling across four independent GEO cohorts, weighted gene co-expression network analysis, multi-database pharmacological target curation, and structure-based molecular docking, provides a level of mechanistic resolution that neither isolated transcriptomic nor single-target approaches can achieve alone.

The present results are consistent with growing evidence indicating that metabolic signaling pathways are deeply intertwined with immune dysregulation in autoimmune thyroid diseases. Previous investigations specifically focused on HT have demonstrated enhanced activation of inflammatory pathways involving STAT1, PI3K/AKT, mTOR, and interferon-responsive genes, which collectively contribute to lymphocytic infiltration and progressive thyrocyte destruction.[13,14] Our identification of MTOR, AKT1, PIK3CA, STAT1, PRKAA1, FOXO3, RPTOR, and ULK1 as central network hubs reinforces the concept that immunometabolic reprogramming is a fundamental component of disease pathogenesis. These observations also align with transcriptomic studies demonstrating extensive activation of cytokine-mediated and T-cell-dependent pathways within HT thyroid tissue.[15]

The enrichment of AMPK and mTOR signaling pathways among the metformin-HT intersection genes further supports previous clinical observations reporting reductions in anti-thyroid antibody titers following metformin therapy.[16] While those studies documented beneficial immunological effects, the molecular basis remained incompletely understood. Our network analysis suggests that the therapeutic activity of metformin may extend beyond systemic metabolic regulation and directly influence intracellular signaling circuits involved in autoimmune maintenance. The convergence of transcriptomic and pharmacological data therefore strengthens the biological plausibility of metformin as a disease-modifying adjunct in HT.

Several mechanisms may explain these observations. AMPK acts as a cellular energy sensor that suppresses anabolic and inflammatory programs under conditions of metabolic stress.[17] Activation of AMPK promotes phosphorylation of RAPTOR and TSC2, resulting in inhibition of mTORC1 activity and downstream suppression of protein synthesis, glycolysis, and inflammatory cytokine production.[18,19] In autoimmune settings, excessive mTOR activation favors differentiation of pathogenic Th1 and Th17 lymphocytes while limiting regulatory T-cell function.[20,21] Experimental evidence indicates that inhibition of the mTOR/HIF-1α axis restores immune tolerance and ameliorates autoimmune thyroiditis by reducing Th17 polarization and promoting Treg expansion.[22] The favorable docking interaction observed between metformin and the AMPKγ1 nucleotide-sensing domain provides a structural rationale for these downstream effects.

Our findings also suggest potential involvement of autophagy-related pathways. ULK1, FOXO3, and other autophagy-associated regulators emerged among the principal network nodes. AMPK-mediated activation of autophagy has been recognized as an important mechanism for controlling immune homeostasis, antigen presentation, and inflammatory signaling.[23,24] Enhanced autophagic activity may contribute to limiting persistent immune activation within the thyroid microenvironment, thereby reducing tissue injury and autoimmune progression.

Notably, ferroptosis emerged as a significantly enriched KEGG pathway among the metformin–HT intersection genes. Ferroptosis is an iron-dependent, regulated form of cell death driven by lipid peroxide accumulation, and recent evidence suggests it may contribute to thyrocyte loss in autoimmune thyroid diseases through oxidative stress-mediated mechanisms. AMPK activation has been shown to suppress ferroptotic signaling via upregulation of GPX4 and inhibition of ACSL4, and metformin has been independently reported to reduce ferroptosis markers in several inflammatory models. While the precise contribution of ferroptosis to HT pathogenesis requires dedicated experimental validation, its identification here warrants further investigation.[25]

Four limitations should be acknowledged. First, this investigation was entirely computational and therefore cannot establish causal biological effects under physiological conditions. Nevertheless, the integration of independent transcriptomic datasets, network analyses, and structure-based docking substantially increases the robustness of the generated hypotheses. Second, molecular docking evaluates binding feasibility rather than actual pharmacodynamic activity; experimental validation of the predicted metformin–AMPKγ1 interaction through biochemical binding assays or cellular AMPK phosphorylation assays is required to confirm these findings. Third, despite ComBat correction, residual batch effects from the integration of microarray and bulk RNA-seq platforms cannot be fully excluded, and the cross-platform $\log_2$FC normalization applied here, while standard, introduces additional analytical assumptions. Fourth, the SwissTargetPrediction probability threshold of ≥ 0.30, while consistent with published network pharmacology practice, may still include low-confidence predictions; sensitivity analyses using stricter thresholds (≥ 0.50) are recommended in future work.

The clinical implications of these observations are noteworthy. Current HT management relies primarily on levothyroxine replacement, which effectively corrects hormonal deficiency but does not directly address the autoimmune process.[26,27] The present findings suggest that metformin may target molecular pathways involved in disease perpetuation, offering a potential adjunctive strategy aimed at immune regulation rather than simple hormone replacement. Future research should focus on experimental validation in cellular and animal models, followed by prospective clinical trials evaluating immunological, biochemical, and histological outcomes in patients with HT.[28,29]

CONCLUSION

This in silico study provides integrated mechanistic evidence that metformin may influence the course of Hashimoto’s thyroiditis through coordinated activation of AMPK-dependent pathways and suppression

of mTOR-centered inflammatory networks. Nine network hub genes, including MTOR, AKT1, and PRKAA1, converged at the metformin–HT pharmacological intersection, and metformin demonstrated thermodynamically favorable binding to AMPKγ1 (ΔG = − 7.4 kcal/mol) and the mTOR kinase domain (ΔG = − 6.1 kcal/mol) in molecular docking simulations. These observations support further experimental validation in thyrocyte and immune cell models, followed by prospective clinical trials evaluating immunological and biochemical outcomes in patients with HT, to determine whether metformin may serve as an effective adjuvant immunomodulatory therapy complementing conventional thyroid hormone replacement.

Declarations

Conflict of Interest:

The authors declare no conflicts of interest.

References

1. Hu X, Chen Y, Shen Y, Tian R, Sheng Y, Que H. Global prevalence and epidemiological trends of Hashimoto's thyroiditis in adults: A systematic review and meta-analysis. Front Public Health. 2022;10:1020709.
2. Zhang QY, Ye XP, Zhou Z, Zhu CF, Li R, Fang Y, et al. Lymphocyte infiltration and thyrocyte destruction are driven by stromal and immune cell components in Hashimoto's thyroiditis. Nat Commun. 2022;13(1):775.
3. Vargas-Uricoechea H. Molecular Mechanisms in Autoimmune Thyroid Disease. Cells. 2023;12(6):918.
4. Bianco AC. Emerging Therapies in Hypothyroidism. Annu Rev Med. 2024;75:307-319.
5. Tywanek E, Michalak A, Świrska J, Zwolak A. Autoimmunity, New Potential Biomarkers and the Thyroid Gland-The Perspective of Hashimoto's Thyroiditis and Its Treatment. Int J Mol Sci. 2024;25(9):4703.
6. Bailey CJ. Metformin: Therapeutic profile in the treatment of type 2 diabetes. Diabetes Obes Metab. 2024;26 Suppl 3:3-19.
7. Nojima I, Wada J. Metformin and Its Immune-Mediated Effects in Various Diseases. Int J Mol Sci. 2023;24(1):755.
8. Ursini F, Russo E, Pellino G, D'Angelo S, Chiaravalloti A, De Sarro G, et al. Metformin and Autoimmunity: A "New Deal" of an Old Drug. Front Immunol. 2018;9:1236.
9. Jia X, Zhai T, Zhang JA. Metformin reduces autoimmune antibody levels in patients with Hashimoto's thyroiditis: A systematic review and meta-analysis. Autoimmunity. 2020;53(6):353-361.

10. Zeng H, Chi H. mTOR signaling in the differentiation and function of regulatory and effector T cells. Curr Opin Immunol. 2017; 46:103-111.
11. Cai T, Du P, Suo L, Jiang X, Qin Q, Song R, et al. High iodine promotes autoimmune thyroid disease by activating hexokinase 3 and inducing polarization of macrophages towards M1. Front Immunol. 2022;13:1009932.
12. Zhao L, Wu Q, Wang X, Wang S, Shi X, Shan Z, et al. Reversal of Abnormal CD4+ T Cell Metabolism Alleviates Thyroiditis by Deactivating the mTOR/HIF1a/Glycolysis Pathway. Front Endocrinol (Lausanne). 2021;12:659738.
13. Chapman NM, Boothby MR, Chi H. Metabolic coordination of T cell quiescence and activation. Nat Rev Immunol. 2020;20(1):55-70.
14. Delgoffe GM, Powell JD. Feeding an army: The metabolism of T cells in activation, anergy, and exhaustion. Mol Immunol. 2015;68(2 Pt C):492-6.
15. Saxton RA, Sabatini DM. mTOR Signaling in Growth, Metabolism, and Disease. Cell. 2017;169(2):361-371.
16. Rena G, Hardie DG, Pearson ER. The mechanisms of action of metformin. Diabetologia. 2017;60(9):1577-1585.
17. Foretz M, Guigas B, Bertrand L, Pollak M, Viollet B. Metformin: from mechanisms of action to therapies. Cell Metab. 2014;20(6):953-66.
18. Viollet B, Guigas B, Sanz Garcia N, Leclerc J, Foretz M, Andreelli F. Cellular and molecular mechanisms of metformin: an overview. Clin Sci (Lond). 2012;122(6):253-70.
19. Kim J, Kundu M, Viollet B, Guan KL. AMPK and mTOR regulate autophagy through direct phosphorylation of Ulk1. Nat Cell Biol. 2011 Feb;13(2):132-41.
20. Herzig S, Shaw RJ. AMPK: guardian of metabolism and mitochondrial homeostasis. Nat Rev Mol Cell Biol. 2018;19(2):121-135.
21. O'Neill LA, Kishton RJ, Rathmell J. A guide to immunometabolism for immunologists. Nat Rev Immunol. 2016;16(9):553-65.
22. Buck MD, O'Sullivan D, Pearce EL. T cell metabolism drives immunity. J Exp Med. 2015;212(9):1345-60.
23. Yang Z, Goronzy JJ, Weyand CM. The glycolytic enzyme PFKFB3/phosphofructokinase regulates autophagy. Autophagy. 2014;10(2):382-3.
24. Deretic V. Autophagy in inflammation, infection, and immunometabolism. Immunity. 2021;54(3):437-453.
25. Sacristán-Gómez P, Delgado-Martín S, Serrano-Somavilla A, Sánchez de la Blanca N, Sampedro-Nuñez M, Sebastian-Valles F, et al. Ferroptosis as a novel alternative cell death model in Hashimoto ´s thyroiditis. Biomed Pharmacother. 2026;198:119276.
26. Jonklaas J, Bianco AC, Bauer AJ, Burman KD, Cappola AR, Celi FS, et al. Guidelines for the treatment of hypothyroidism. Thyroid. 2014;24(12):1670–1751.

27. Davis MG, Phillippi JC. Hypothyroidism: Diagnosis and Evidence-Based Treatment. J Midwifery Womens Health. 2022;67(3):394-397.
28. Perl A. Activation of mTOR (mechanistic target of rapamycin) in rheumatic diseases. Nat Rev Rheumatol. 2016;12(3):169-182.
29. Chi H. Regulation and function of mTOR signalling in T cell fate decisions. Nat Rev Immunol. 2012;12(5):325-338.

Figures

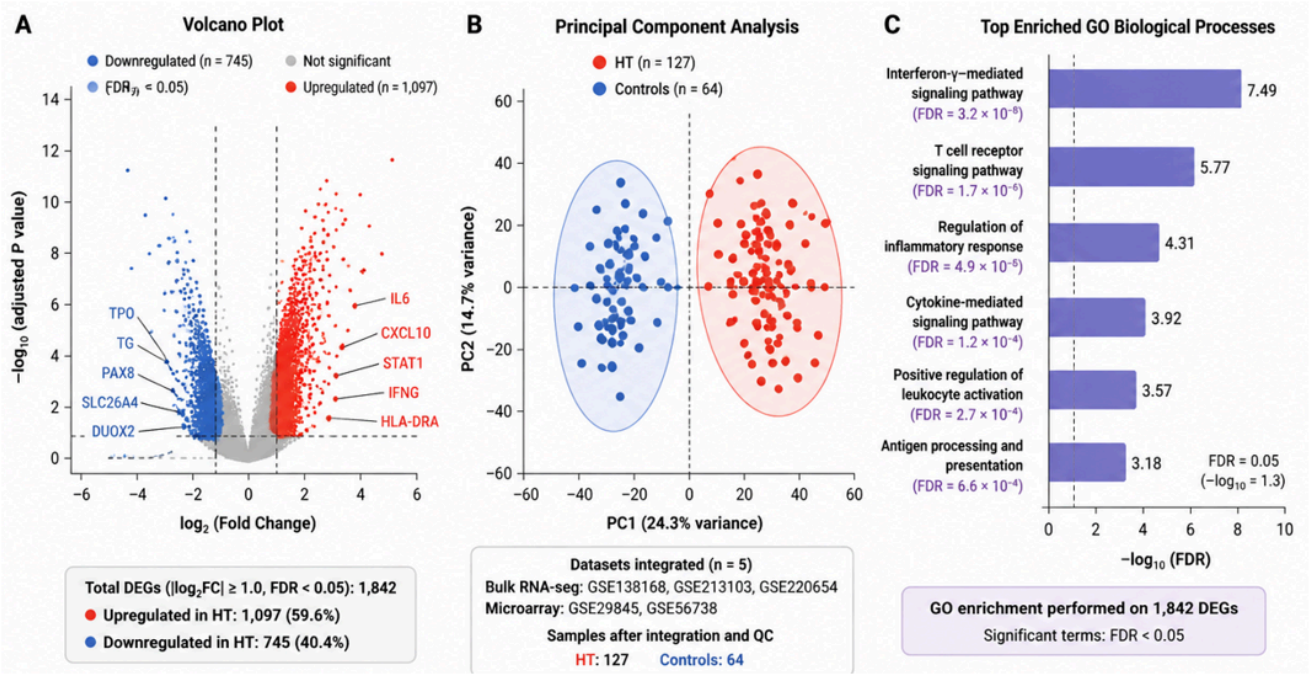


Figure 1

Transcriptomic landscape of Hashimoto's thyroiditis showing PCA, volcano plot, and enriched biological pathways

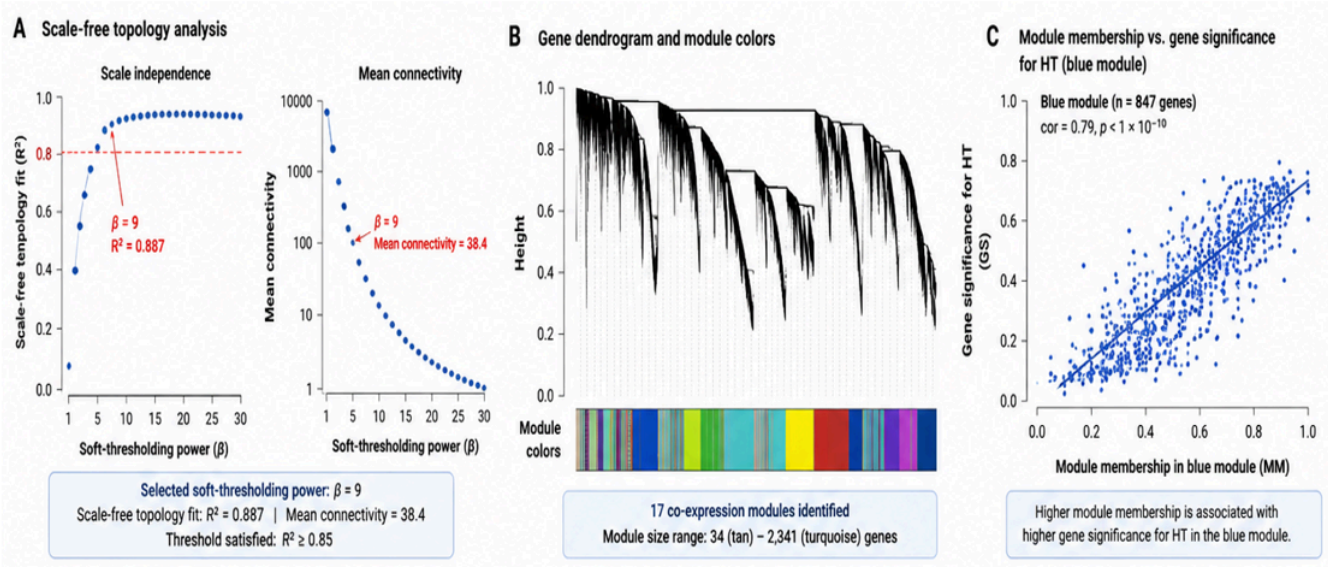


Figure 2

WGCNA Co-expression network analysis of integrated thyroid transcriptome

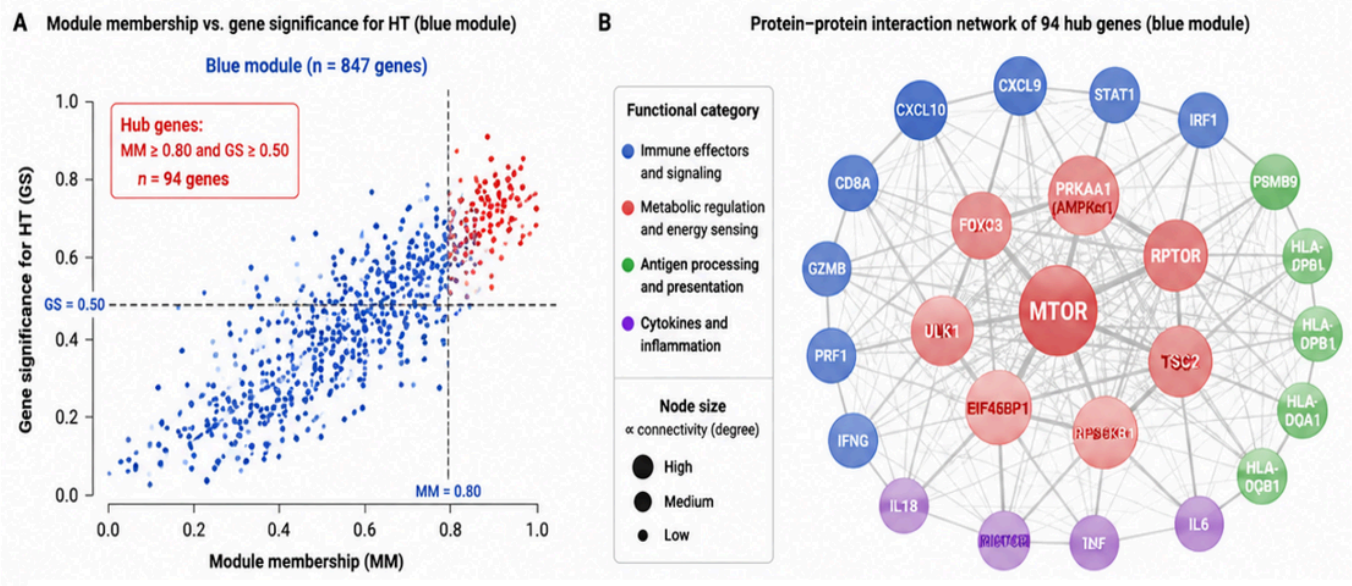


Figure 3

Immune-metabolic hub genes in the blue co-expression module

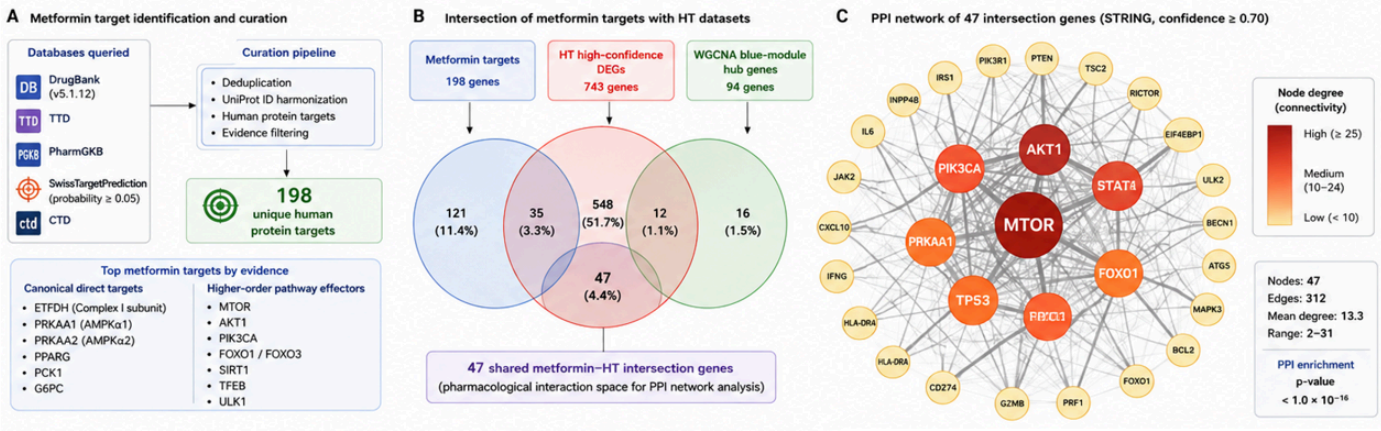


Figure 4

Network pharmacology and identification of key Metformin-HT intersection targets

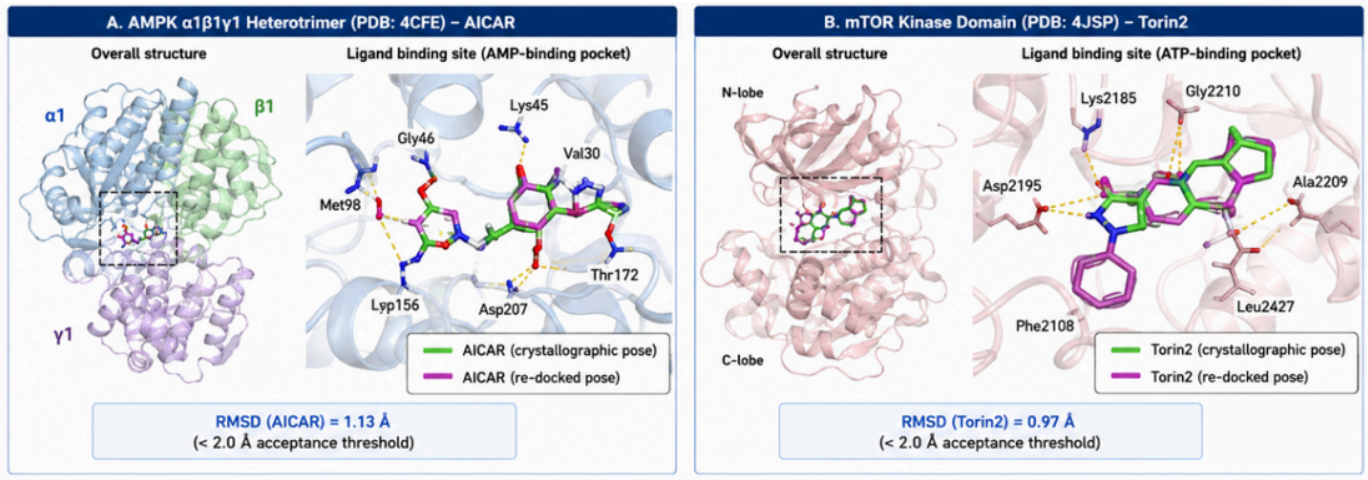


Figure 5

Protocol validation: Re-docking of native co-crystallized ligands

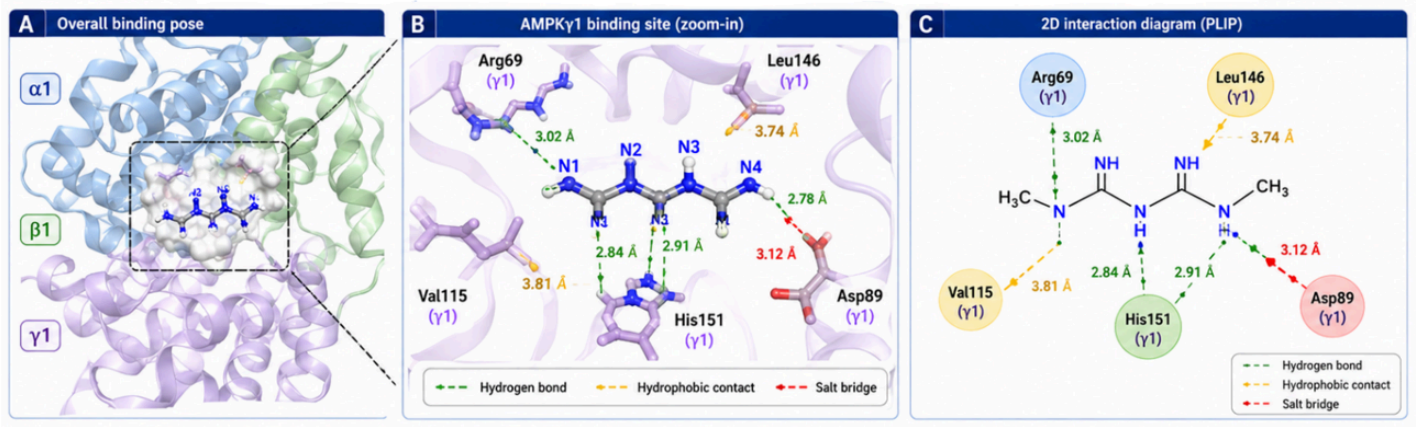


Figure 6

PLIP interaction profiling of metformin within the AMPK α1β1γ1 heterotrimer

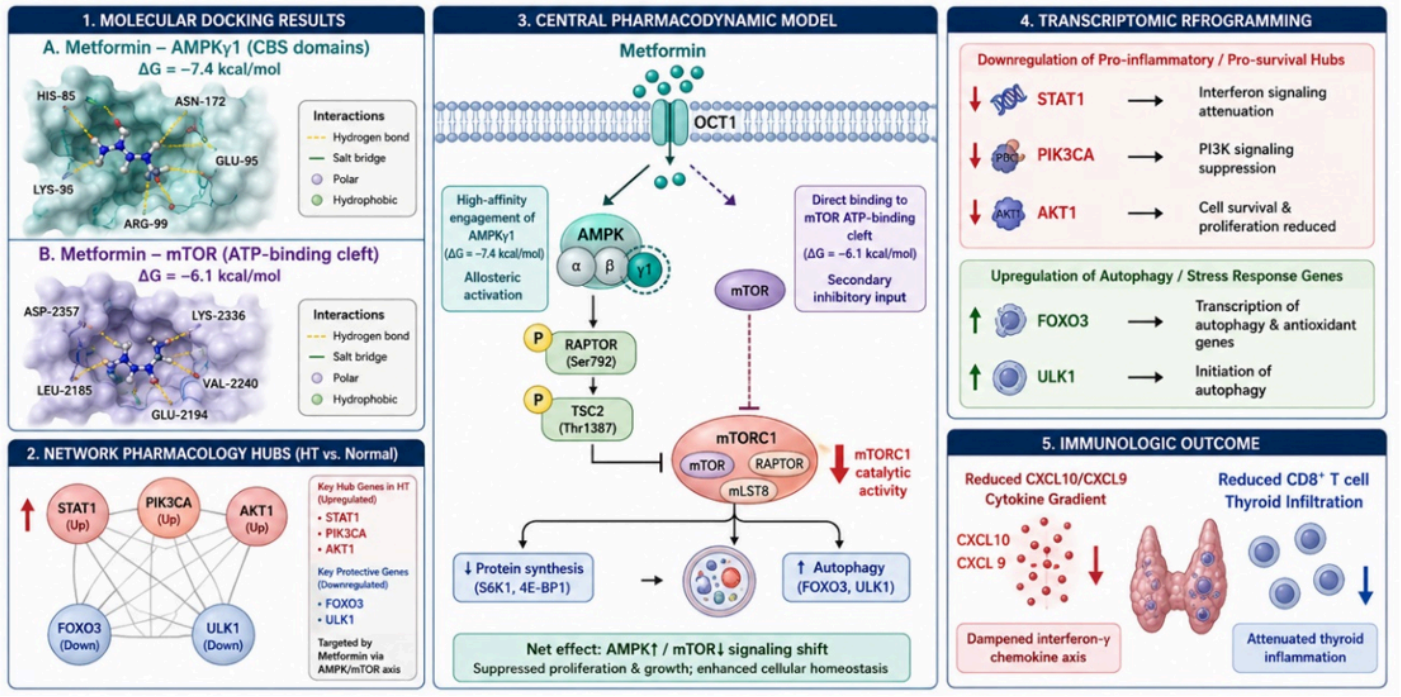


Figure 7

Integrated pharmacodynamic model of metformin in HT thyroid disease